# Copper Nanocluster and Pollutant Analysis

Copper nanoclusters (Cu NCs) with their inherent optical and chemical advantages have gained increasing attention as a kind of novel material that possesses great potential, primarily in the use of contaminants sensing and bio-imaging. With a focus on environmental safety, this article comprehensively reviews the recent advances of Cu NCs in the application of various contaminants, including pesticide residues, heavy metal ions, sulfide ions and nitroaromatics. The common preparation methods and sensing mechanisms are summarized.

## 1. Introduction

Metal nanoclusters (MNCs) with ultra-small and tunable sizes, excellent photoluminescent efficiency, long fluorescence lifespan, desirable physical and biochemical stability and relatively low toxicity, have prompted the great advancement of research in both theoretical and practical fields [1][2]. The last decade witnessed the successful synthesis of novel MNCs and their applications in fluorescent sensors mainly based on gold (Au) and silver (Ag) nanoclusters. Meanwhile, copper nanoclusters (Cu NCs) have gradually gained increasing attention due to their chemical similarity with Ag NCs and Au NCs, distinct fluorescent characteristics, and in particular the low-cost and easier accessibility of their precursors as well as facile preparation procedures [3][4]. With the help of various functional ligands, it is possible to tune their emission wavelengths and obtain highly photoluminescent nanoclusters, providing potential for large-scale applications. More importantly, Cu NCs possess additional merits over other noble metal clusters with their excellent biocompatibility [5][6]. The fluorescent probes based on Cu NCs have demonstrated their versatility in sensing, lighting and bioimaging in clinical diagnosis and treatment [6][7][8][9]. Meanwhile, the significance of monitoring and analyzing various contaminants for the purpose of environmental safety should also be emphasized due to the widespread application of Cu NCs in this field.

In this entry, we emphasize the recent progress of Cu NCs for application in environmental analysis. We first make a brief introduction of the common synthesis approaches of Cu NCs with a highlight on their intriguing optical properties. In the second section, we categorize the mainstream strategies based on Cu NCs in terms of sensing mechanisms. In the following part, we mainly present several typical novel Cu NCs targeting various contaminants in the environment, including pesticides, heavy metals, sulfide anions, as well as aromatic compounds. In the end, we conclude the article by discussing the challenges and prospects in the future development of Cu NCs as sensors for environmental pollutants.

## 2. Preparation Methods and Sensing Mechanism of Cu NCs

Many research groups developed GSH capped Cu NCs with orange or red fluorescence emission [10][11][12]. A one-pot sonochemical synthesis method was established for the preparation of GSH-Cu NCs by Wang et al. [13]. In this method, Cu (NO 3) 2 and GSH were mixed in water by 1: 4 ratio, and the pH of solution was adjusted to 6 with NaOH. The reaction was conducted in 15 min via ultrasonic irradiation, which is facile, fast and easy to operate. The as-synthesized GSH-Cu NCs exhibits bright red luminescence at λ max = 606 nm and quantum yield up to 5.3%. As mentioned above, there are also many fluorescent GSH-Cu NCs that have been reported with blue emission. The main difference in the synthesis process is that red emitting GSH-Cu NCs utilized GSH as both a stabilizing and a reducing agent in acidic condition, while blue emitting ones were synthesized in basic condition or reduced by AA. DNA template is also frequently exploited in the fabrication of Cu NCs with red emission [14][15][16][17]. Li et al. developed copper nanoclusters templated by poly(thymine)-DNA with a fluorescence emission of 627 nm [18]. The DNA-Cu NCs were produced by a facile reaction between copper sulfate and poly-T DNA in 3-(N-morpholino) propanesulfonic acid buffer with the help of sodium ascorbate. Intriguingly, a research group successfully synthesized Cu NCs with strong orange emission utilized egg white as template [19]. The formation of Cu NCs relies on the interaction between multiple functional groups in egg white and CuSO 4. Hydrazine hydrate was employed as reducing agent and NaOH was used to provide the basic environment. The reaction proceeded extremely fast, since it is carried out under microwave.
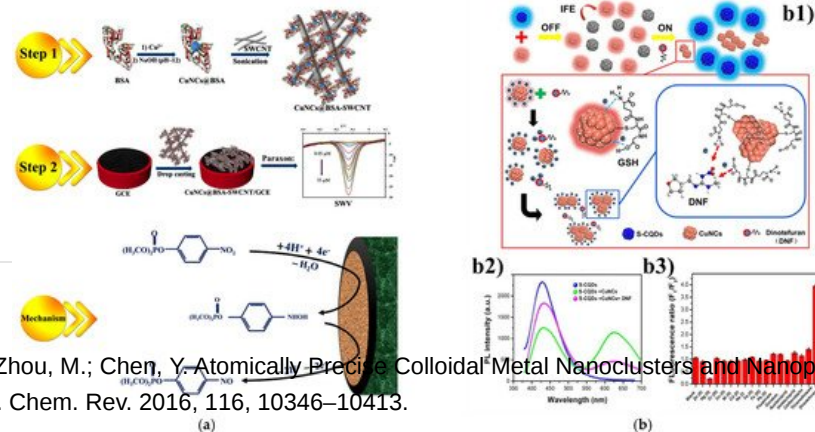
On account of the prominent fluorescence property and cost-effectiveness of Cu NCs, numerous Cu NCs-based sensing probes have been developed for multitude of analytes. The majority of Cu NCs-based fluorescent sensors follow turn-off mechanism that the analytes are detected due to the decrease in fluorescence intensity.

Inner filter effect (IFE) is a most common strategy in the development of turn-off sensors [20][21][22][23]. The inner filter effect refers to the fluorescence quenching process that the quencher absorbs the emission or excitation light of fluorophore. A study in this context established a label-free assay for nitrofurantoin using adenosine-stabilized Cu NCs [24]. Nitrofurantoin's UV absorption band located at 250–430 nm happens to overlap the Cu NCs' fluorescence excitation and emission spectra. In this way, the excitation and emission light could be shielded by nitrofurantoin, leading to decrease in fluorescence intensity.

Ratiometric fluorescence sensors have also attracted increasing research interest since it exhibits dominant advantages in accuracy, sensitivity and stability. In a ratiometric sensing approach, the detection is achieved by the intensity ratio of dual-emission peaks, which could eliminate the interference of environment and probe concentrations by self-calibration. A CuNC@AF660 sensor was fabricated for ratiometric sensing of calcium ions. The fluorescence intensity of Cu NCs emission peak was enhanced gradually with the increase in Ca 2+ concentration through ion-induced AIE mechanism. The Alex Fluor 660 NHS ester fabricated on Cu NCs provides the inner-reference signal.

# 3. Sensing Applications Based on Cu NCs

In this section, we mainly highlight the Cu NCs-based detection systems targeting common pesticides ( **Table 1** ), e.g., paraoxon, dinotefuran (DNF), o-phenylenediamine (OPD), dithiocarbamates (DTCs), thiram, paraquat, fluazina, nitrofurantoin (NFT). Copper nanocluster was employed in the construction of an enzyme-free electrochemical biosensor toward paraoxon as the model of organophosphates (OP) [25]. The biocompatible nanocomposite Cu NCs@BSA-SWCNT was synthesized by combining bovine serum albumin (BSA) template-capped Cu nanoclusters (Cu NCs@BSA) and single-walled carbon nanotubes (SWCNT), which demonstrated remarkable sensitivity and high electrocatalytic property toward the reduction of paraoxon ( **Figure 1** a). The entrapped Cu NCs rendered high electrical conductivity and concentrated the redox active centers on the surface of the probe, while the SWCNT further enhanced the electrocatalytic activity along with conductivity of the glassy carbon electrode (GCE) surface. The linear range was 0.5–35 µM, with a limit of detection of 12.8 nM. Moreover, this electrochemical nanocomposite was found to be able to effectively determine paraoxon with satisfied recoveries ranged from 93% to 104% in a real water sample. In order to detect and monitor the residues of dinotefuran (DNF), which has been widely used in agriculture, novel sensing probes and platforms based on fluorescent copper nanoclusters have been constructed. Yang et al. [26] established a dual-emission ratiometric fluorescent probe by integrating sulfur-doped carbon quantum dots (S-CQDs) and Cu NCs with mixed fluorescent signals ( **Figure 1** b). The as-developed hybrid (S-CQDs/Cu NCs) was observed to demonstrate desirable sensitivity and selectivity towards DNF with linear range from 10 to 500 µM. In this nanocomposite, IFE caused the decrease in fluorescent signals of S-CQDs with the addition of Cu NCs. In the presence of dinitefuran, the IFE between S-CQDs and Cu NCs would be weakened due to the aggregation of Cu NCs, leading to the restoration of S-CODs fluorescence. In the case of honey as the real sample, this ratiometric fluorescent S-CQDs/Cu NCs showed good analysis performance for the detection of DNF. Besides, another ratiometric detection system was proposed for o-phenylenediamine (OPD) based on the use of copper nanoclusters [27]. This method achieved signal amplification and ideal sensitivity through the combined influence of the oxidation reaction and FRET effect. With addition of OPD into Cu NCs, the fluorescence intensity of the Cu NCs at 432 nm decreased, while the oxidized OPD (oxOPD) showed strong fluorescence at 557 nm. This detection strategy was able to determine OPD in real water samples with an ultralow limit of detection of 0.096 g L −1 . Furthermore, a rapid and sensitive detection method of dithiocarbamates (DTCs) with dual functionality in fluorescence and colorimetry was established utilizing CTAB -entrapped Cu NCs [28]. Owing to the fluorescence quenching of the Cu NCs with addition of DTCs, the detection system demonstrated remarkable sensitivity and selectivity toward DTCs with a linear range from 1 to 100 mg kg −1 and a low limit of detection of 0.63 mg kg −1 .

**Figure 1.** (a) Schematic representation of the fabrication and suggested mechanism for paraoxon reduction; (b) (b1) The schematic illustration of ratiometric determination of dinotefuran based on S-CQDs/CuNCs probe; (b2) the emission spectra of S-CQDs and S-CQDs/CuNCs with and without the addition of DNF; (b3) selectivity analyses of as-developed ratiometric fluorescent probe mixed various interfering chemicals.

**Table 1.** List of fluorescent probes based on Cu NCs for pesticide detection.

| No | Analytes | Sensors | Em. Maxima (nm) | Sensing Mechanism | Linear Range | Limit of Detection (LOD) | Real Sample | Ref. |
|----|----------|---------|-----------------|-------------------|--------------|--------------------------|-------------|------|
| 1 | Paraoxon | Cu NCs @ BSA-SWCNT/GCE | 325/420 | electrochemical method | 0.05–0.5 µM 0.5–35 µM | 12.8 nM | water | [25] |
| 2 | Thiram Paraquat | Egg white- Cu NCs | 344/600 | turn off | 0.5–1000 µM 0.2–1000 µM | 70 nM 49 nM | water | [19] |
| 3 | Metham sodium | CTAB-Cu NCs | 254/620 | fluorescent based colorimetric method | 1–100 mg kg⁻¹ | 0.63 mg kg⁻¹ | apple, pear and cherry tomato | [28] |
| 4 | Thiram | Cu-GSH NCs | 365/497 | turn on | 0.05–25 µM | 1.4 nM | pears and cabbage | [29] |
| 5 | o-Phenylenediamine | GSH-Cu NCs | 334/438 | ratiometric | 0.15–110 µg L⁻¹ | 83 ng L⁻¹ | industry water | [27] |
| 6 | Nitrofurantoin | Adenosine-Cu NCs | 285/437 | turn off | 0.05–4.0 µM | 30 nM | lake water | [24] |
| 7 | Dinotefuran | S-CQDs/Cu NCs | 330/420 | ratiometric | 10–500 µM | 7.04 µM | honey | [26] |
| 8 | AChE Methamidophos | DNA-Cu/Ag NCs | 480/565 | turn off turn on | 0.05–2.0 U⁻¹ | 0.05 UL⁻¹ 0.075 mg L⁻¹ (IC₅₀) | water and vegetable | [30] |
| 10 | AChE | L-His-Cu/Ag NCs | 390/485 | turn off | 0.1–1.0 UL⁻¹ and 1.0–7.0 UL⁻¹ | 0.03 UL⁻¹ | — | [31] |
| 9 | AChE | PVP-Cu NCs | 370/438 | ratiometric | 2.0–70 UL⁻¹ | 0.56 UL⁻¹ | human serum sample | [32] |
| 10 | AChE | PEI-Cu NCs | 365/495 | turn on | 3–200 UL⁻¹ | 1.38 UL⁻¹ | human serum sample | [33] |

Heavy metals are notorious and hazardous contaminants in environment due to their low degradability, acute toxicity, high bioaccumulation, and other factors. Here, we summarized and highlighted representative strategies for CuNCs-based determination of several representative heavy metal ions including mercury ions (Hg2+), lead ions (Pb2+), chromate anions (CrO₄²⁻), and copper ions (Cu2+) (**Table 2** ).

## References

1. Jin, R.; Zeng, C.; Zhou, M.; Chen, Y. Atomically Precise Colloidal Metal Nanoclusters and Nanoparticles: Fundamentals and Opportunities. Chem. Rev. 2016, 116, 10346–10413.

2. Du, Y.; Sheng, H.; Astruc, D.; Zhu, M. Atomically Precise Noble Metal Nanoclusters as Efficient Catalysts: A Bridge between Structure and Properties. Chem. Rev. 2019, 120, 526–622.

3. Liu, X.; Astruc, D. Atomically precise copper nanoclusters and their applications. Coord. Chem. Rev. 2018, 359, 112–126.

4. Wang, Z.; Chen, B.; Rogach, A.L. Synthesis, optical properties and applications of light-emitting copper nanoclusters. Nanoscale Horiz. 2017, 2, 135–146.

5. Baghdasaryan, A.; Bürgi, T. Copper nanoclusters: Designed synthesis, structural diversity, and multiplatform applications. Nanoscale 2021, 13, 6283–6340.

6. Lai, W.F.; Wong, W.T.; Rogach, A.L. Development of Copper Nanoclusters for In Vitro and In Vivo Theranostic Applications. Adv. Mater. 2020, 32, 1906872.

7. Shahsavari, S.; Hadian-Ghazvini, S.; Hooriabad Saboor, F.; Menbari Oskouie, I.; Hasany, M.; Simchi, A.; Rogach, A.L. Ligand functionalized copper nanoclusters for versatile applications in catalysis, sensing, bioimaging, and optoelectronics. Mater. Chem. Front. 2019, 3, 2326–2356.

8. Hu, X.; Liu, T.; Zhuang, Y.; Wang, W.; Li, Y.; Fan, W.; Huang, Y. Recent advances in the analytical applications of copper nanoclusters. TrAC Trends Anal. Chem. 2016, 77, 66–75.

9. An, Y.; Ren, Y.; Bick, M.; Dudek, A.; Waworuntu, E.H.; Tang, J.; Chen, J.; Chang, B. Highly fluorescent copper nanoclusters for sensing and bioimaging. Biosens. Bioelectron. 2020, 154, 112078.

10. Wang, Z.; Chen, R.; Xiong, Y.; Cepe, K.; Schneider, J.; Zboril, R.; Lee, C.-S.; Rogach, A.L. Incorporating Copper Nanoclusters into Metal-Organic Frameworks: Confinement-Assisted Emission Enhancement and Application for Trinitrotoluene Detection. Part. Part. Syst. Charact. 2017, 34, 1700029.

11. Patel, R.; Bothra, S.; Kumar, R.; Crisponi, G.; Sahoo, S.K. Pyridoxamine driven selective turn-off detection of picric acid using glutathione stabilized fluorescent copper nanoclusters and its applications with chemically modified cellulose strips. Biosens. Bioelectron. 2018, 102, 196–203.

12. Shen, Z.; Zhang, C.; Yu, X.L.; Li, J.; Liu, B.H.; Zhang, Z.P. A facile stage for Cu2+ ions detection by formation and aggregation of Cu nanoclusters. Microchem. 2019, 145, 517–522.

13. Wang, C.; Cheng, H.; Huang, Y.; Xu, Z.; Lin, H.; Zhang, C. Facile sonochemical synthesis of pH-responsive copper nanoclusters for selective and sensitive detection of Pb2+ in living cells. Analyst 2015, 140, 5634–5639.

14. Li, J.; Fu, W.; Bao, J.; Wang, Z.; Dai, Z. Fluorescence Regulation of Copper Nanoclusters via DNA Template Manipulation toward Design of a High Signal-to-Noise Ratio Biosensor. ACS Appl. Mater. Interfaces 2018, 10, 6965–6971.

15. He, J.-L.; Wang, X.-X.; Mei, T.-T.; Wu, L.; Zeng, J.-L.; Wang, J.-H.; Wang, J.; Yu, D.; Cao, Z. DNA-templated copper nanoclusters obtained via TdT isothermal nucleic acid amplification for mercury(ii) assay. Anal. Methods 2019, 11, 4165–4172.

16. Su, Y.-T.; Lan, G.-Y.; Chen, W.-Y.; Chang, H.-T. Detection of Copper Ions Through Recovery of the Fluorescence of DNA-Templated Copper/Silver Nanoclusters in the Presence of Mercaptopropionic Acid. Anal. Chem. 2010, 82, 8566–8572.

17. Ou, L.J.; Huang, J.K.; Lv, X.L.; Huang, N. DsDNA-templated fluorescent copper nanoclusters for ultrasensitive label-free detection of Pb2+ ion. Chin. J. Anal. Lab. 2016, 35, 899–902.

18. Jia, H.; Chang, J.; Zhou, T.; Li, H. A facile, sensitive, and highly specific trophic CuNCs for the determination of acid induction and mercury ions (Hg 2+) based on DNA-templated copper nanoclusters. Talanta 2016, 160, 475–480.

Table 2. A list of Fluorescent probes based on Cu NCs for Hg detection.

| No | Analytes | Sensors | Ex./Em. Maxima (nm) | Sensing Mechanism | Linear Range | Limit of Detection (LOD) | Real Sample | Ref. |
|---|---|---|---|---|---|---|---|---|
| 1 | Hg²⁺ | Cu NCs@P-8B | 400/535 | turn off | 10–100 μM | 10 μM | aqueous solution | [34] |
| 2 | Hg²⁺ | Curcuminoids-Cu NCs | 350/440 | turn off | 0.5 nM–25 μM | 0.12 nM | water | [35] |
| 3 | Hg²⁺ | Cu NCs | 340/560 | turn off | 7–40 μM | 23 nM | water | [36] |
| 4 | Hg²⁺ | Trypsin-Cu NCs | 360/567 | turn off | 0.1–100 μM | 30 nM | human urine and serum samples | [37] |
| 5 | Hg²⁺ | TdT-INAA-DNA-Cu NCs | 343/600 | turn off | 0.2–500 nM | 76 pM | environmental water | [15] |
| 6 | Hg²⁺ | GSH–Cu NCs | 360/445 | turn off | 10 nM–10 μM | 3.3 nM | water and rice | [38] |
| 7 | Hg²⁺ | poly(mT)-DNA Cu NCs | 340/650 | turn on | 50 pM–2.5 μM and 2.5–500 μM | 16 pM | lake water | [14] |
| 8 | Hg²⁺ | DTT-Cu NCs/CNNS nanocomposite | 395/615 | electrochemiluminescence | 0.05–10 nM | 0.01 nM | lake and tap water | [39] |
| 9 | Hg²⁺ | Metallothionein–Cu NCs | | UV-VIS | 97 nm–2.3 μM and 15.6 μM | 43.8 nM | environmental water | [40] |
| 10 | Hg²⁺ | GSH-Cu NCs | 375/440 | turn off | 0.04–60 μM | 22 nM | water | [41] |
| 11 | Hg²⁺ | Cytosine rich-ssDNA-Cu/Ag NCs | 470/550 | turn off | 40–550 nM | 2.4 nM | lake and tap water | [42] |
| 12 | Hg²⁺ | apt-Cu@Au NCs | 470/656 | ratiometric | 0.5–9 μM | 4.92 nM | porphyra | [43] |
| 13 | Hg²⁺ | 4-chlorothiophenol-Cu NCs | 330/605 | turn off | 1–500 nM | 0.3 nM | environmental water | [44] |
| 14 | Hg²⁺ | Bsa-Cu NCs | 320/420 | turn off | 0.01–10 μM | 4.7 nM | water | [45] |
| 15 | Hg²⁺ | BSA-Cu NCs | 395/645 | turn off | 20–1000 nM | 0.2 nM | — | [46] |
| 16 | Hg²⁺ | L-Cys-Cu NCs | 375/480 | turn off | 0.1–1000 μM | 24 nM | human urine sample | [47] |
| 17 | Hg²⁺ | dsDNA-Cu NCs | 570/595 | turn off | 0.04–8 nM | 4 pM | water | [48] |
| 18 | Hg²⁺ | Ag/Cu NCs | colorimetric | turn on | 2.1–91 nM | 0.05 nM | aqueous sample | [49] |
| 19 | Hg⁺ | CDs-CuNCs | 345/430,647 | ratiometric | 0–4000 nM | 0.31 nM | Tap, lake water | [50] |

19. ... Kailasa, S.K. One-step green synthetic approach for the preparation of multicolor emitting copper nanoclusters and their applications in chemical species sensing and bioimaging. Biosens. Bioelectron. 2016, 80, 243–248.

20. Dong, W.; Sun, C.; Sun, M.; Ge, H.; Asiri, A.M.; Marwani, H.M.; Ni, R.; Wang, S. Fluorescent Copper Nanoclusters for the Iodide-Enhanced Detection of Hypochlorous Acid. ACS Appl. Nano Mater. 2019, 3, 312–318.

21. Shojaeifard, Z.; Heidari, N.; Hemmateenejad, B. Bimetallic AuCu nanoclusters-based florescent chemosensor for sensitive detection of Fe(3+) in environmental and biological systems. Spectrochim. Acta. Part A Mol. Biomol. Spectrosc. 2019, 209, 202–208.

22. Luo, M.; Wei, J.; Zhao, Y.; Sun, Y.; Liang, H.; Wang, S.; Li, P. Fluorescent and visual detection of methyl-paraoxon by using boron-and nitrogen-doped carbon dots. Microchem. J. 2020, 154, 104547.

23. Wei, J.; Yang, Y.; Dong, J.; Wang, S.; Li, P. Fluorometric determination of pesticides and organophosphates using nanoceria as a phosphatase mimic and an inner filter effect on carbon nanodots. Microchim. Acta 2019, 186, 66.

24. Wang, Y.; Chen, T.; Zhuang, Q.; Ni, Y. Label-free photoluminescence assay for nitrofurantoin detection in lake water samples using adenosine-stabilized copper nanoclusters as nanoprobes. Talanta 2018, 179, 409–413.

25. Bagheri, H.; Afkhami, A.; Khoshsafar, H.; Hajian, A.; Shahriyari, A. Protein capped Cu nanoclusters-swcnt nanocomposite as a novel candidate of high performance platform for organophosphates enzymeless biosensor. Biosens. Bioelectron. 2017, 89, 829–836.

26. Yang, Y.; Wei, Q.; Zou, T.; Kong, Y.; Su, L.; Ma, D.; Wang, Y. Dual-emission ratiometric fluorescent detection of dinotefuran based on nitrogen-doped carbon quantum dots and copper nanocluster hybrid. Sens. Actuators B Chem. 2020, 321, 128534.

27. Ma, Y.; Yu, Y.; Lin, B.; Zhang, L.; Cao, Y.; Guo, M. A novel signal amplification strategy based on the use of copper nanoclusters for ratiometric fluorimetric determination of o-phenylenediamine. Mikrochim. Acta 2019, 186, 206.

28. Chen, S.; Wang, ... Specific detection and discrimination of dithiocarbamates using CTAB-encapsulated fluorescent copper nanoclusters. Talanta 2020, 210, 120627.

29. Li, L.; Hou, C.; Li, J.; Yang, Y.; Hou, J.; Ma, Y.; He, Q.; Luo, H.; Huo, D. Fluazinam direct detection based on the inner filter effect using a copper nanocluster fluorescent probe. Anal. Methods 2019, 11, 4637–4643.

30. Li, W.; Li, W.; Hu, Y.; Xia, Y.; Shen, Q.; Nie, Z.; Huang, Y.; Yao, S. A fluorometric assay for acetylcholinesterase activity and inhibitor detection based on DNA-templated copper/silver nanoclusters. Biosens. Bioelectron. 2013, 47, 345–349.

31. Li, Y.; Hu, Y.; He, Y.; Ge, Y.; Song, G.; Zhou, J. Sensitive Naked-eye and Fluorescence Determination of Acetylcholinesterase Activity using Cu/Ag Nanoclusters Based on Inner Filter Effect. ChemistrySelect 2019, 4, 7639–7644.

32. Wang, M.; Liu, L.; Xie, X.; Zhou, X.; Lin, Z.; Su, X. Single-atom iron containing nanozyme with peroxidase-like activity and copper nanoclusters based ratio fluorescent strategy for acetylcholinesterase activity sensing. Sens. Actuators B Chem. 2020, 313, 128023.

33. Yang, J.; Song, N.; Lv, X.; Jia, Q. UV-light-induced synthesis of PEI-CuNCs based on Cu2+-quenched fluorescence turn-on assay for sensitive detection of biothiols, acetylcholinesterase activity and inhibitor. Sens. Actuators B Chem. 2018, 259, 226–232.

34. Benavides, J.; Quijada-Garrido, I.; García, O. The synthesis of switch-off fluorescent water-stable copper nanocluster Hg(2+) sensors via a simple one-pot approach by an in situ metal reduction strategy in the presence of a thiolated polymer ligand template. Nanoscale 2020, 12, 944–955.

35. Bhamore, J.R.; Deshmukh, B.; Haran, V.; Jha, S.; Singhal, R.K.; Lenka, N.; Kailasa, S.K.; Murthy, Z.V.P. One-step eco-friendly approach for the fabrication of synergistically engineered fluorescent copper nanoclusters: Sensing of Hg2+ ion and cellular uptake and bioimaging properties. New J. Chem. 2018, 42, 1510–1520.

36. Cai, Z.; Zhu, R.; Pang, S.; Tian, F.; Zhang, C. One-step Green Synthetic Approach for the Preparation of Orange Light Emitting Copper Nanoclusters for Sensitive Detection of Mercury(II) Ions. ChemistrySelect 2020, 5, 165–170.

37. Feng, J.; Chen, Y.; Han, Y.; Liu, J.; Ma, S.; Zhang, H.; Chen, X. pH-Regulated Synthesis of Trypsin-Templated Copper Nanoclusters with Blue and Yellow Fluorescent Emission. ACS Omega 2017, 2, 9109–9117.

38. Hu, X.; Wang, W.; Huang, Y. Copper nanocluster-based fluorescent probe for sensitive and selective detection of Hg(2+) in water and food stuff. Talanta 2016, 154, 409–415.

39. Liu, H.; Gao, X.; Zhuang, X.; Tian, C.; Wang, Z.; Li, Y.; Rogach, A.L. A specific electrochemiluminescence sensor for selective and ultra-sensitive mercury(ii) detection based on dithiothreitol functionalized copper nanocluster/carbon nitride nanocomposites. Analyst 2019, 144, 4425–4431.

| N | target Analytes | | Ex/Em Maxima (nm) | Sensing Mechanism | Linear Range | Limit of Detection (LOD) | Real Sample | Ref. |
|---|---|---|---|---|---|---|---|---|
| 20 | $Hg^{2+}$ | BSA-CuNCs/ BSA-AuNCs | 365/398,616 | ratiometric | 0.06–1 µM and 1–4 µM | 19.4 nM | Tap, mineral, lake water | [51] |
| 21 | $Pb^{2+}$ | BSA-Cu NCs | 324/401 (fluorescence), 324/396 (light scattering) | turn on | 30–180 nM; 3–21 nM | 10 nM; 1 nM | environmental water | [52] |
| 22 | $Pb^{2+}$ | BSA-Cu NCs | 325/410 | turn off | 0–200 nM | — | — | [53] |
| 23 | $Pb^{2+}$ | GSH-Cu NCs | 360/607 | turn on | 200–700 µM | 106 µM | water | [54] |
| 24 | $Pb^{2+}$ | Cu NCs-GNQDs | 365/468,632 | ratiometric | 0.01–2.5 mg L$^{-1}$ | 0.0031 mg L$^{-1}$ | porphyra | [55] |
| 25 | $Pb^{2+}$ | Metallothionein–Cu NCs | — | turn on | 0.7–96 µM | 1.5 nM | environmental water | [40] |
| 26 | $Pb^{2+}$ | dsDNA-Cu NCs | 340/605 | turn off | 0–150 µM | 5.2 nM | tap water | [17] |
| 27 | $Pb^{2+}$ | GSH-Cu NCs | 420/606 | turn off | 1–160 nM | 1 nM | — | [13] |
| 28 | $Pb^{2+}$ | Cu NASs | 340/590 | turn off | 2–100 nM | 0.75 nM | aqueous sample | [56] |
| 29 | $Cr_2O_7$ | GSH@CDs-Cu NCs | 360/450,750 | ratiometric | 0–20 µM | 0.9 µM | tap water, spring water samples and human urine | [57] |
| 30 | Cr(VI) | PAMP-Cu NCs | 357/428 | turn off | 0–150 µM | 8.5 µM | water | [58] |
| 31 | Cr(VI) | Thiosalicylic acid/Cysteamine Cu NCs | 355/411 | turn off | 0.1–1000 µM | 30 nM | Water | [59] |
| 32 | Cr(VI) | Cysteamine-Au/Cu NCs | 350/436 | turn off | 0.2–100 µM | 80 nM | water and human urine sample | [60] |
| 33 | Cr(VI) | Cu NCs@TA | 360/430 | turn off | 0.03–60 µM | 5 nM | water sample | [61] |
| 34 | $Cu^{2+}$ | D-Penicillamine - Cu NCs | 391/673 | turn on | 0.95–6.35 ppm | 0.3 ppm | tap water | [62] |
| 35 | $Cu^{2+}$ | CdSe QDs @ hPEI-Cu NCs | 380/495,625 | ratiometric | 0.022–8.8 µM | 8.9 nM | river water | [63] |
| 36 | $Cu^{2+}$ | GSH-Cu NCs | 330/615 | turn on | 0.25–10 µM | 170 nM | chalcocite | [12] |
| 37 | $Cu^{2+}$ | DNA-Cu/Ag NCs | 480/570 | turn off | 5–200 nM | 2.1 nM | soil and pond water | [16] |
| 38 | $Cu^{2+}$ | Cytidine-Cu NCs | 300/380 | turn on | 0.05–20 µM | 32 nM | lake water | [64] |
| 39 | $Cu^{2+}$ | BSA-Cu NCs | 340/420 | turn off | 0.02–34 µM | 1 nM | tap water | [65] |
| 40 | $Cu^{2+}$ | BSA-Cu NCs/ BSA-Au NCs | 365/398,616 | ratiometric | 0.1–1 µM and 1–5 µM | 23.4 nM | Tap, mineral, lake water | [51] |

40. Liu, R.; Zuo, L.; Huang, X.; Liu, S.; Yang, G.; Li, S.; Lv, C. Colorimetric determination of lead(II) or mercury(II) based on target-induced switching of the enzyme-like activity of metallothionein-stabilized copper nanoclusters. Microchim. Acta 2019, 186, 250.

41. Luo, T.; Zhang, S.; Wang, Y.; Wang, M.; Liao, M.; Kou, X. Glutathione-stabilized Cu nanocluster-based fluorescent probe for sensitive and selective detection of Hg2+ in water. Luminescence 2017, 32, 1092–1099.

42. Mao, A.; Wei, C. Cytosine-rich ssDNA-templated fluorescent silver and copper/silver nanoclusters: Optical properties and sensitive detection for mercury(II). Mikrochim. Acta 2019, 186, 541.

43. Shi, Y.; Li, W.; Feng, X.; Lin, L.; Nie, P.; Shi, J.; Zou, X.; He, Y. Sensing of mercury ions in Porphyra by Copper @ Gold nanoclusters based ratiometric fluorescent aptasensor. Food Chem. 2021, 344, 128694.

44. Wang, H.-B.; Bai, H.-Y.; Wang, Y.-S.; Gan, T.; Liu, Y.-M. Highly selective fluorimetric and colorimetric sensing of mercury(II) by exploiting the self-assembly-induced emission of 4-chlorothiophenol capped copper nanoclusters. Microchim. Acta 2020, 187.

45. Xiaoqing, L.; Ruiyi, L.; Zaijun, L.; Xiulan, S.; Zhouping, W.; Junkang, L. Fast synthesis of copper nanoclusters through the use of hydrogen peroxide additive and their application for the fluorescence detection of Hg2+ in water samples. New J. Chem. 2015, 39, 5240–5248.

46. Xu, J.; Han, B. Synthesis of Protein-Directed Orange/Red-Emitting Copper Nanoclusters via Hydroxylamine Hydrochloride Reduction Approach and Their Applications on Hg2+ Sensing. Nano 2016, 11, 1650108.

47. Yang, X.; Feng, Y.; Zhu, S.; Luo, Y.; Zhuo, Y.; Dou, Y. One-step synthesis and applications of fluorescent Cu nanoclusters stabilized by l-cysteine in aqueous solution. Anal. Chim. Acta 2014, 847, 49–54.

48. Zhang, H.; Guan, Y.; Li, X.; Lian, L.; Wang, X.; Gao, W.; Zhu, B.; Liu, X.; Lou, D. Ultrasensitive Biosensor for Detection of Mercury(II) Ions Based on DNA-Cu Nanoclusters and Exonuclease III-assisted Signal Amplification. Anal. Sci. 2018, 34, 1155–1161.

49. Cai, Y.; Wang, J.; Niu, L.; Zhang, Y.; Liu, X.; Liu, C.; Yang, S.; Qi, H.; Liu, A. Selective colorimetric sensing of sub-nanomolar Hg2+ based on Hg2+-stimulated enhancing peroxidase mimics of silver/copper nanoclusters. Analyst 2021, 146, 4630–4635.

50. Li, Z.; Pang, S.; Wang, M.; Wu, M.; Li, P.; Bai, J.; Yang, X. Dual-emission carbon dots-copper nanoclusters ratiometric photoluminescent nano-composites for highly sensitive and selective detection of Hg2+. Ceram. Int. 2021, 47, 18238–18245.

51. Zhong, J.; Hao, J.; Jiang, Y.; Wang, H.; Jia, R. Synthesis of dual-emissive ratiometric probe of BSA-Au NCs and BSA-Cu NCs and their sensitive and selective detection of copper and mercury ions. J. Photochem. Photobiol. A Chem. 2021, 408.

52. Feng, D.-Q.; Zhu, W.; Wang, W. Dual-modal light scattering and fluorometric detection of lead ion by stimuli-responsive aggregation of BSA-stabilized copper nanoclusters. RSC Adv. 2016, 6, 96729–96734.

53. Goswami, N.; Giri, A.; Bootharaju, M.S.; Xavier, P.L.; Pradeep, T.; Pal, S.K. Copper Quantum Clusters in Protein Matrix: Potential Sensor of Pb2+ Ion. Anal. Chem. 2011, 83, 9676–9680.

54. Han, B.Y.; Hou, X.; Xiang, R.-C.; Yu, T.-B.; Li, Y.; Peng, T.; He, G.-H. Detection of Lead Ion Based on Aggregation-induced Emission of Copper Nanoclusters. Chin. J. Anal. Chem. 2017, 45, 23–27.

55. Li, W.; Wu, X.; Li, Q.; Shi, Y.; Zhai, X.; Yin, L.; Li, Z.; Huang, X.; Wang, X.; Shi, J.; et al. Copper nanoclusters @ nitrogen-doped carbon quantum dots-based ratiometric fluorescence probe for lead (II) ions detection in porphyra. Food Chem. 2020, 320, 126623.

56. Li, M.; Cai, Y.; Peng, C.; Wei, X.; Wang, Z. DNA dendrimer–templated copper nanoparticles: Self-assembly, aggregation-induced emission enhancement and sensing of lead ions. Microchim. Acta 2021, 188.

57. Bai, H.; Tu, Z.; Liu, Y.; Tai, Q.; Guo, Z.; Liu, S. Dual-emission carbon dots-stabilized copper nanoclusters for ratiometric and visual detection of Cr2O7(2−) ions and Cd(2+) ions. J. Hazard. Mater. 2020, 386, 121654.

58. Khonkayan, K.; Sansuk, S.; Srijaranai, S.; Tuntulani, T.; Saiyasombat, C.; Busayaporn, W.; Ngeontae, W. New approach for detection of chromate ion by preconcentration with mixed metal hydroxide coupled with fluorescence sensing of copper nanoclusters. Microchim. Acta 2017, 184, 2965–2974.

59. Lin, Y.-S.; Chiu, T.-C.; Hu, C.-C. Fluorescence-tunable copper nanoclusters and their application in hexavalent chromium sensing. RSC Adv. 2019, 9, 9228–9234.

60. Shellaiah, M.; Simon, T.; Thirumalaivasan, N.; Sun, K.W.; Ko, F.H.; Wu, S.P. Cysteamine-capped gold-copper nanoclusters for fluorometric determination and imaging of chromium(VI) and dopamine. Mikrochim. Acta 2019, 186, 788.

60. Chcani, X.; Bai, W.; Liu, S.; ... Extensive use of fluorescence measuring for the production and release ... chromium ions based on copper nanoclusters. Luminescence 2020, 86, 289–296.

62. Li, D.; Li, B.; Yang, S.H. A selective fluorescence turn-on sensing system for evaluation of Cu2+ polluted water based on ultra-fast formation of fluorescent copper nanoclusters. Anal. Methods 2015, 7, 2278–2282.

63. Liu, Z.C.; Qi, J.W.; Hu, C.; Zhang, L.; Song, W.; Liang, R.P.; Qiu, J.D. Cu nanoclusters-based ratiometric fluorescence probe for ratiometric and visualization detection of copper ions. Anal. Chim. Acta 2015, 895, 95–103.

64. Wang, Y.; Chen, T.; Zhang, Z.; Ni, Y. Cytidine-stabilized copper nanoclusters as a fluorescent probe for sensing of copper ions and hemin. RSC Adv. 2018, 8, 9057–9062.

65. Zhong, Y.; Zhu, J.; Wang, Q.; He, Y.; Ge, Y.; Song, C. Copper nanoclusters ... Microchim. Acta 2015, 182, 909–915.

66. Maayan, G.; Behar, A.E.; Sabater, L.; Baskin, M.; Hureau, C. A Water-Soluble Peptoid Chelator that Can Remove Cu2+ from Amyloid-β and Stop the Formation of Reactive Oxygen Species Associated with Alzheimer's Disease. Angew. Chem. Int. Ed. 2021, 60, 2–12.

67. Migliorini, C.; Porciatti, E.; Luczkowski, M.; Valensin, D. Structural characterization of Cu2+, Ni2+ and Zn2+ binding sites of model peptides associated with neurodegenerative diseases. Coord. Chem. Rev. 2012, 256, 352–368.

The prevalence of copper ion residues in the food and in the environment is another looming danger due to damage to the human liver and the nervous system caused by excessive Cu 2 + . Typically, Alzheimer's disease (AD), as a common neurodegenerative disease, might be caused by excessive accumulation of copper ion and corresponding oxidative stress [66][67]. Hyperbranched polyethyleneimine-protected copper nanoclusters (hPEI-Cu NCs) were integrated with the silica-coated CdSe quantum dots (QDs) to obtain a novel ratiometric and visual analytical probe toward copper ions through the simple and green one-pot chemical reduction method at room temperature [63]. This QDs@Cu NCs probe exhibited high sensitivity and visual detection capability toward Cu 2 + , which could be attributed to the self-calibration function of the dual-emission fluorescence signals inherent in the ratio-based fluorescence probe. The fluorescence of hPEI-Cu NCs was quenched due to the interaction of its amine groups with Cu 2+ , while the fluorescence intensity of QDs remained unchanged, and the distinct color changes could be easily observed by the naked eye under the UV-light. The linear range of the probe in Cu 2+ concentrations was, approximately, from 22 nM to 8.8 μM, with an estimated detection limit of 8.9 nM ( **Figure 5** b). When applied in the real water samples with different concentrations of Cu 2 + , the as-synthesized probe exhibited satisfactory recovery.

## 4. Conclusions and Perspectives

This entry summarized and reported the latest development of fluorescent copper nanoclusters utilized in monitoring various types of environmental contaminants. Despite the fascinating advances, there is still a long and arduous way ahead in further improving Cu NCs to make them ideal materials for pollutant detection, quantitative determination, and, even, decomposition and removal. Firstly, the sizes of the current Cu NCs designed fall into a rather wide range, and the desirable optical properties of most Cu NCs heavily rely on excitation. Both of these two aspects may largely constrain the possibility of efficient application of Cu NCs in environmental analysis on a large scale. Secondly, efforts are imperative to further enhance the chemical and optical stability, as well as quantum yield of Cu NCs, so as to improve their feasibility as sensors in more complex, real environments, even with complicated, interfering factors. Lastly, the functions of the current probes are expected to be extended from pure detection of environmental pollutants to simultaneous detection, degradation and, even, removal.